



Contents lists available at ScienceDirect

Advanced Drug Delivery Reviews

journal homepage: www.elsevier.com/locate/addr

Investigation of endosome and lysosome biology by ultra pH-sensitive nanoprobes[☆]

Chensu Wang ^{a,b}, Tian Zhao ^a, Yang Li ^a, Gang Huang ^a, Michael A. White ^b, Jinming Gao ^{a,*}^a Department of Pharmacology, Simmons Comprehensive Cancer Center, University of Texas Southwestern Medical Center, 5323 Harry Hines Blvd, Dallas, TX 75390, USA^b Department of Cell Biology, University of Texas Southwestern Medical Center, 5323 Harry Hines Blvd, Dallas, TX 75390, USA

ARTICLE INFO

Article history:

Received 2 June 2016

Received in revised form 29 August 2016

Accepted 30 August 2016

Available online xxxx

Keywords:

Endocytic organelles

pH sensitive nanoprobes

Organelle imaging

pH buffering

Cell signaling

Metabolomics

ABSTRACT

Endosomes and lysosomes play a critical role in various aspects of cell physiology such as nutrient sensing, receptor recycling, protein/lipid catabolism, and cell death. In drug delivery, endosomal release of therapeutic payloads from nanocarriers is also important in achieving efficient delivery of drugs to reach their intracellular targets. Recently, we invented a library of ultra pH-sensitive (UPS) nanoprobes with exquisite fluorescence response to subtle pH changes. The UPS nanoprobes also displayed strong pH-specific buffer effect over small molecular bases with broad pH responses (e.g., chloroquine and NH₄Cl). Tunable pH transitions from 7.4 to 4.0 of UPS nanoprobes cover the entire physiological pH of endocytic organelles (e.g., early and late endosomes) and lysosomes. These unique physico-chemical properties of UPS nanoprobes allowed a 'detection and perturbation' strategy for the investigation of luminal pH in cell signaling and metabolism, which introduces a nanotechnology-enabled paradigm for the biological studies of endosomes and lysosomes.

© 2016 Published by Elsevier B.V.

Contents

1. Introduction of endosome/lysosome biology	0
1.1. Characteristics of endocytic organelles	0
1.2. The physiological importance of pH in endo/lysosomal maturation and function	0
2. pH-sensitive nanomaterials	0
3. A novel ultra pH-sensitive (UPS) nanoprobe for 'detecting and perturbing' endo/lysosomes	0
3.1. Lighting up endocytic organelles	0
3.1.1. Sharp OFF/ON response rendered by micellization and homo-FRET effect	0
3.1.2. Activation of UPS nanoprobes in specific endocytic organelles	0
3.1.3. An ultra pH-sensitive polymer library	0
3.2. Quantitative measurements: an 'always-ON/OFF-ON' design	0
3.3. Buffering effect – 'detecting and perturbing'	0
3.3.1. Physico-chemical and in vitro characterization	0
3.3.2. Coat protein dynamics	0
3.3.3. Cell signaling and metabolism	0
3.3.4. Selective killing of cancer cells	0
4. Conclusions and future prospects	0
Acknowledgments	0
References	0

1. Introduction of endosome/lysosome biology

☆ This review is part of the *Advanced Drug Delivery Reviews* theme issue on "Molecular Imaging".

* Corresponding author.

E-mail address: jinming.gao@utsouthwestern.edu (J. Gao).

Endocytosis is involved in various important cellular processes, such as protein/lipid metabolism, antigen presentation and energy homeostasis [1,2]. Endocytosis process senses and regulates the interaction

between a cell and its external environment. For example, the recycling and degradation of transmembrane receptors through endocytosis regulates the sensitivity of cells to their specific ligands [3]. Extracellular materials, including a variety of molecules, cargos and fluid-phase contents, are internalized by cells through endocytosis. They travel along the increasingly acidic endocytic pathway and end up in endosomes or lysosomes. pH homeostasis and maintenance of proton gradient across organelle membranes are essential to cell physiology [1]. For endocytic pathways, progressive acidification is essential to various aspects of different biochemical and physiological functions [4,5]. For instance, it compartmentalizes ligand–receptor uncoupling and activation of proteases for protein/lipid degradations into endosomes and lysosomes, respectively.

Lysosomes, as the 'end-point' of the endocytic pathway, were first discovered by Christian de Duve in 1955 [6]. Lysosomes have a highly acid lumen with various kinds of hydrolases/lipases for protein/lipid degradation and recycling of extracellular and intracellular components via endocytosis and autophagy, respectively. The resulting breakdown products become building blocks for protein/lipid synthesis and energy generation. More recently, lysosomes have been identified as signaling organelles that play an important role in nutrient sensing and response [7,8], and activate a master gene that regulates nutrient and energy metabolism [9,10].

1.1. Characteristics of endocytic organelles

After receptors and their ligands are internalized into cells through clathrin-coated pits (~100 nm diameter) [11] or early endosomes, they are disassociated from each other because of the acidic environment in the early endosomes. Most membrane-bound receptors are recycled back to cell surface for another round of delivery, while the ligands are destined for degradation in lysosomes. Many ligand-conjugated nanoparticle designs took advantage of receptor-mediated endocytosis for targeted delivery into endocytic organelles. For non-targeted nanoparticles, most are internalized into cells through micropinocytosis, or fluidic phase endocytosis. It occurs with cell membrane ruffling and forms a pocket (up to 5 μ m diameter) [12] engulfing bulk of extracellular fluids and molecules. The macropinosomes then pinch off from cell membrane and fuse with endosomes and lysosomes.

Late endosomes (250–400 nm diameter) [5] are bigger than early endosomes in size. Some late endosomes have more complex internal vesicular structures and are also named as multivesicular bodies (MVBs). The MVBs comprise inward invaginations of late endosome membranes and may contain certain receptors. In general, late endosomes are closer to nucleus than early endosomes, and they have extensive exchange with trans-Golgi-network (TGN). Lysosomal hydrolases are carried to late endosomes from TGN through mannose-6-phosphate receptors. Once the hydrolases are released, the receptor is retrieved to the Golgi by retromer and Rab9 [13]. Along with further drop of luminal pH, late endosomes mature into lysosomes. Lysosomes appear as electron dense bodies when viewed under electron microscopy. They are highly heterogeneous in terms of composition, morphology and density mainly due to the diversity of cargos and their degradation levels.

Rab GTPases, a family of small GTPases that regulate membrane trafficking, have been found to be the most important biomarkers for organelle identity and regulators of the endocytic pathway [13]. Rab GTPases are associated with cell/organelle membranes when they are in the guanine triphosphate (GTP)-binding 'ON' form and they will be removed when in the guanine diphosphate (GDP)-binding 'OFF' form. Rab5 is a biomarker for early endosomes, because normally Rab5-GDP resides in the cytosol, and its guanine-nucleotide exchange factors (GEFs) activate it to GTP-binding form on early endosome membranes. Rab4 and Rab11 are also early endosome markers, but Rab11 is mainly located on recycling endosome membranes. Maturation of early endosomes to late endosomes involves a switch from Rab5 to Rab7

that also mediates the fusion with lysosomes [3]. Another late endosome biomarker, Rab9, mediates the trafficking between late endosomes and TGN. Lysosomes are enriched in a family of glycosylated lysosome associated membrane proteins (LAMPs), so Rab7 and LAMPs are both markers for them. Although these membrane proteins are useful markers of organelle identity, since endocytic organelles are highly dynamic, and there is extensive traffic among them, it is possible that none of these proteins are exclusively associated with any of these components. Multiple characterizations may be needed in some cases.

The machinery of lysosomal biogenesis was unclear for a long time until recently a specific gene network called coordinated lysosomal expression and regulation (CLEAR) was identified. Most lysosomal genes share a common CLEAR sequence (GTCACGTGAC) close to the transcriptional start site, which mediates transcriptional activation [14]. The transcriptional factor EB (TFEB) can bind to this sequence and induce the transcription of lysosomal genes. When lysosomes are under stress, TFEB translocates from cytoplasm to nucleus and activates its target genes. Thus, TFEB is considered as the master regulator of lysosomal biogenesis and function, which coordinates the transcription of lysosomal genes. Recently, it has also been found to regulate starvation-induced autophagy and lipid metabolism [15], placing the lysosomal network in the center of cell metabolism and homeostasis.

1.2. The physiological importance of pH in endo/lysosomal maturation and function

Acidification is substantial to endosome maturation. Endocytic vesicles are more acidic than a lot of other organelles, and lysosomal pH values can be as low as 4.0–4.5 [4]. The low pH not only offered an optimal environment for hydrolase activation, it is also essential for uncoupling ligands from receptors, inactivation of microbicidal factors, membrane trafficking, cargo transportation and other important reactions. The primary way of delivering protons into the organelle lumen is through proton-pumping vacuolar-ATPase (v-ATPase) [4]. V-ATPase are composed of two distinct subunits: a transmembrane V_0 complex that transfers protons across membranes and a V_1 cytosolic complex that hydrolyzes ATP and converts chemical energy into mechanical force required for proton displacement. Na^+/K^+ ATPase, Cl^- and Ca^{2+} channels that influx counter ions or efflux cations are also in place to maintain the balance of membrane potential and pH [16–18].

Cargo release, hydrolase maturation, degradation, autophagy and intracellular trafficking are all dependent on pH gradients [17]. Bafilomycin A1 (bafA1) [19] and concanamycins [20] are specific inhibitors of v-ATPase and can efficiently dissipate the proton gradient across organelle membranes of the whole endocytic pathway. Baf A1 is sufficient to block the transportation of cargos from early endosomes to late endosomes in most cases indicating a defect of endosome maturation [21,22]. It has also been used to block the fusion of late endosomes [23] or autophagosomes [24] with lysosomes indicating an important role that luminal pH plays in cargo transportation.

In the therapeutics of diseases with disturbed lysosomal pH, restoring the acidity of endo/lysosomes could be an efficient way to promote the degradation and clearance of accumulated substances. Presenelin-1 is an important protein in Alzheimer's disease, and it has also been shown to regulate the trafficking of v-ATPase to lysosomal membranes [25]. Mutated presenelin-1 is one of the major causes of familial Alzheimer's disease, which results in disrupted lysosomal pH, defective hydrolase maturation and activity that may be attributed to abnormal v-ATPase trafficking [25].

Defective or blocked endocytic pathways and/or global disturbance of intracellular pH have been associated with a variety of pathological conditions [4,26], such as oncogenic transformation [27], autoimmune disease [28] and neurodegenerative diseases [29,30]. However, specific knowledge is still lacking on how local (i.e., organelle-specific) pH variations may affect cell physiology. The biochemical functions of many membrane-bound proteins are highly sensitive to minor pH

perturbations (e.g., H^+ -sensing G protein-coupled receptors [31] and vacuolar H^+ -ATPase (v-ATPase) a2-isoform [32]), which leads to the hypothesis that luminal pH can impact a variety of cell signaling processes and cellular metabolism. Currently, various reagents have been used to manipulate and study the acidification of endocytic organelles, which include lysosomotropic agents (e.g., chloroquine and NH_4Cl), v-ATPase inhibitors (e.g., baflomycin A1) and ionophores (e.g., nigericin and monensin) [33]. However, these reagents are membrane permeable and may simultaneously target multiple acidic organelles (e.g., Golgi apparatus with a pH of ~6.5) [1], and therefore, are not specific to inhibit catabolic organelles along the endocytic pathway. Typically, the luminal pH of endocytic organelles are measured by small molecular pH sensors such as Lysotracker and Lysosensor probes. These probes accumulate in acid organelles and exhibit pH-dependent fluorescence increase. However, the pH-dependent fluorescence change is relatively low (<20 fold), which also results in a wide pH-response range (usually spans over 2 pH units) thereby a low pH resolution. Moreover, the small molecular probes with low protonation degree may diffuse back into cytosol and increase background fluorescence or accumulate in other acidic organelles such as Golgi. These limitations have motivated us to design and develop alternative pH-sensitive probes to label endosomes and lysosomes. pH-sensitive polymer nanoparticles represent a new set of tools for studying endocytic organelles since they are exclusively taken up by endocytosis. These nanoparticles are versatile in specific controls in particle size, surface charge and modification to further increase specific targeting to a particular cell-surface receptor. In addition, the nanoparticles can be tailored to target a predetermined pH to respond to a specific endocytic pH as a binary off/on sensor. These potential advantages endow unique opportunities to nanoparticles in organelle imaging, drug/gene delivery and other cell biology studies.

2. pH-sensitive nanomaterials

pH-sensitive small molecules have been used to detect and study the acidification of endocytic organelles for a long time, such as Lysotracker, Lysosensor and fluorescein, but they suffer from low pH resolution and off-target effect as described above. Currently, various pH-sensitive nanomaterials have been developed by employing molecular moieties with pK_a values around the functional pH range of endo/lysosomes [34].

Typical pH-sensitive groups including those containing tertiary amines, carboxylic acids, sulfonamide, and amino acids (especially histidine) exhibit protonated and deprotonated states [35–37]. For polymer nanoparticles, typical examples of monomers include acrylic acid, methacrylic acid, maleic anhydride, N,N-dimethylaminoethyl methacrylate. A dramatic conformational change of micelles and a swelling behavior of hydrogels according to their protonation state are commonly exploited to show pH transitions [38]. A typical example of this design is the poly-L-histidine (polyHis) micelles developed by Bae and co-workers [39–42]. The polyHis has a pK_b around neutral pH and the unsaturated nitrogen offers an amphoteric property by protonation and deprotonation. The micelles were stable at pH 8.0 and started to disassociate when pH drops below 7.4. In order to tailor the triggering pH of polyHis micelles to more acidic pH and also to make it more stable, Bae and coworkers developed a mixed micelle composed of poly(L-histidine)-poly(ethylene glycol) block copolymers (polyHis-*b*-PEG) and poly(L-lactide) (PLLA)-*b*-PEG. It is stable at pH above 7.4 and undergoes a dramatic structural change upon a pH drop to 6.8–7.0 [39], which can be activated in early endosome and/or acidic tumor microenvironment. An anti-cancer drug doxorubicin (DOX) was successfully encapsulated into the micelle core due to the hydrophobic interaction with deprotonated polyHis segments. A selective disassociation at acidic (~pH 6.8) tumor microenvironment endows an improved anti-tumor efficacy of the mixed micelles versus the pH-insensitive PLLA-*b*-PEG micelles alone [43]. Sulfonamide is another example of pH-sensitive groups used in polymers because of the pK_a (6.8–6.9) of the sulfonamide groups

close to the physiological pH. When pH is higher than 6.8, the negatively charged poly(methacryloyl sulfadimethoxine) (PSD)-*b*-PEG interacts with positively charged DNA-containing polycation complex through electrostatic interactions; when pH drops below 6.8, PSD-*b*-PEG detached from the complex because the sulfonamide groups were no longer charged [44]. The shielding effect from PSD-*b*-PEG offers an opportunity for the protection of ligand-decorated nanoparticles before the environment becomes acidic [45].

Another strategy is to introduce acid-labile linkages into the system. These chemical bonds, such as acyl hydrazone, acetals and 2,3-dimethylmaleic amide (DMMA) linkages [46], are stable at neutral pH (i.e. pH 7.2–7.4), but undergo acid-catalyzed cleavage when pH drops. The Park and Kataoka groups have used this approach to attach the anti-cancer drugs to the copolymers with acid-labile acyl hydrazone linkages [47,48]. Hydrolysis of hydrazone bonds in lysosomes (pH 5.0 or lower) facilitates a controlled release of drugs from the core of polymer micelles. Fréchet and coworkers have introduced another design of pH-sensitive micelles by attaching hydrophobic groups to the periphery of dendrimer blocks by an acid-sensitive acetal linkage [49,50]. Hydrolysis of acetal linkages at low pH, including tumor tissue and/or endocytic organelles, causes disassociation of hydrophobic groups, and the dendrimer core becomes hydrophilic, which destabilizes the micelle and facilitates the drug release causing a similar cytotoxicity to that of the free drug. Unlike most pH-sensitive linkages that requires highly acidic environment such as lysosomes to induce cleavage, DMMA was found to be selectively cleaved at weakly acidic pH like tumor microenvironment by Wang and coworkers [51]. They developed a cross-reacted nanogel composed of poly(2-aminoethyl methacrylate hydrochloride) (PAMA) and DMMA. The nanogel was negatively charged due to the carboxylate group on DMMA at neutral pH, after cleavage at lower pH (6.8), the positively charged amine groups were left, contributing to more interaction of the nanogels with cell membranes and enhanced cell uptake. The charge conversion from negative to positive values when pH is more acidic also contributes to an accelerated drug (DOX) release probably due to the decreased interaction between DOX and the protonated nanogels.

The success of these pH-sensitive polymer nanomaterials in drug/gene delivery depends on the progressive decomposition of polymers/micelles and the slow but sustained release of therapeutic agents at tumor site, which may take up to days. In these cases, even a fast release takes minutes to occur [39]. However, they may not be the best choice in terms of imaging, especially live-cell imaging of highly dynamic endocytic organelles. Moreover, most of these materials are limited by their near neutral pK_a , which does not have the bandwidths for imaging endocytic organelles with luminal pH ranges from 4.0 to 6.8. Therefore, ultra pH-sensitive nanomaterials that respond sharply to subtle pH changes and have a tunable, broad pH-sensing range are needed to fill in the gap.

3. A novel ultra pH-sensitive (UPS) nanoprobe for 'detecting and perturbing' endo/lysosomes

3.1. Lighting up endocytic organelles

During the maturation process of endosomes to lysosomes, a drop of luminal pH from 7.4 to 6.5 can occur in a few minutes, and 6.5 to 4.0 can be within 1 h [3]. To track the dramatic pH change within a relatively short time period, it requires the nanoprobe to be ultra pH-sensitive and render a fast temporal response. Fluorescence is one of the most common readouts for cell/organelle imaging. A system with non-linear signal amplification and high detection sensitivity is preferred to precisely report the pH changes and to facilitate further quantification.

3.1.1. Sharp OFF/ON response rendered by micellization and homo-FRET effect

To achieve sharp pH-sensitivity and fast response, a series of copolymers with ionizable tertiary amine groups and covalently conjugated

fluorophores have been developed [36] (Fig. 1a–b). In this ultra pH-sensitive (UPS) nanoprobe design, poly(ethylene glycol) (PEO) is used as the hydrophilic segment while ionizable tertiary amines are introduced into the hydrophobic segment (PR). When conjugating pH-insensitive dyes with small Stokes shift (<40 nm) into the PR segment, the dyes stay silent in the core of the micelle at higher pH predominantly through homo-FRET (Förster resonance energy transfer) [52,53] decay mechanism between the dye molecules. When pH drops below the transition pH, protonated and positively charged PR segment causes micelle disassembly and increase of fluorescence emission due to the diminished homo-FRET induce quenching.

Mechanistic investigation shows that the self-assembled micelles drive reversible catastrophic, all-or-nothing protonation of tertiary amine groups, leading to rapid and complete dissociation of the micelles within a narrow pH range (e.g., <0.3 pH unit) [54]. The significantly sharpened pH response and binary on/off transition arises from the strong hydrophobic pH cooperativity induced by hydrophobic micellization, which is absent in unimolecular (e.g., chloroquine) and commonly used polymeric bases (e.g., poly(ethyleneimines)). Combination of theoretical modeling and experimental validation revealed key structural parameters such as repeating unit hydrophobicity and polymer chain length, which impact pKa and pH transition sharpness of UPS nanoprobes [54,55]. The cooperativity and fluorescence activation make fluorescence a perfect readout of pH response and extends the application of the nanoprobes to *in vitro* imaging, especially for specific endocytic compartments [56].

3.1.2. Activation of UPS nanoprobes in specific endocytic organelles

The hydrophobicity of the PR segment and the resulting transition pH of the UPS nanoprobes can be adjusted by altering the monomers used for the PR segment. For example, in the linear dialkyl series, isopropyl (UPS_{6.2}, each subscript indicates the pK_a of the corresponding copolymer) and butyl (UPS_{5.3}) groups yield a distinctive transition pH at 6.2 and 5.3, respectively, which is ideal to differentiate the luminal pH of early endosomes (6.0–6.5) [57] and late endosomes/lysosomes

(5.0–5.5) [4,57]. When co-incubating with human H2009 lung cancer cells, UPS nanoprobes showed no observable fluorescence signal in the medium at pH 7.4 [36]. At 15 min, fluorescent signal from UPS_{6.2}-TMR started to increase over time, and after 30 min, co-localization of UPS_{6.2}-TMR and green fluorescent protein (GFP)-labeled Rab5a (an early endosome marker) can be found in 80% of cells, while only 12% co-localization with GFP-fused LAMP1 (a lysosome marker) were observed at the same time (Fig. 1c). In contrast, UPS_{5.3}-TMR nanoprobes showed a different distribution for activation. Along the whole time, less than 10% of co-localization with GFP-Rab5a was observed. Instead, almost all of the activated UPS_{5.3}-TMR nanoprobes ended up in GFP-LAMP1-positive organelles (Fig. 1d). A vacuolar-ATPase inhibitor baf A1, which blocks proton pumping and acidification of endocytic organelles, is able to abolish the intracellular activation of both UPS nanoprobes. The selective activation of UPS_{6.2} and UPS_{5.3} in early endosomes and lysosomes reveals an early indication of this non-linear OFF/ON nanoprobe system for studying the maturation of endocytic organelles.

3.1.3. An ultra pH-sensitive polymer library

In the previous UPS nanoprobe design, the transition pH of different nanoprobes is controlled by the hydrophobicity of PR segments synthesized from different single monomers. The drawback of this strategy is that the transition pH is limited by the discrete hydrophobicity of the PR segments. To continuously fine tune the transition pH of the UPS nanoprobes, a random copolymerization strategy was employed by adjusting the molar fraction of two monomers with different but closely matched hydrophobicity [58] (Fig. 2b). A list of methacrylate monomers with different side chains, including ethyl, propyl, butyl and pentyl groups, were used. The resulting nanoprobe series consist of 10 nanoprobes with 0.3 pH increment covering the entire physiological pH range from 4.0 to 7.4. Each nanoprobe maintains a sharp pH response within 0.25 pH range. To label the nanoprobe library with a wide range of fluorophores (400–820 nm), the pH-insensitive fluorophore series also need to be extended from those with small Stokes shifts

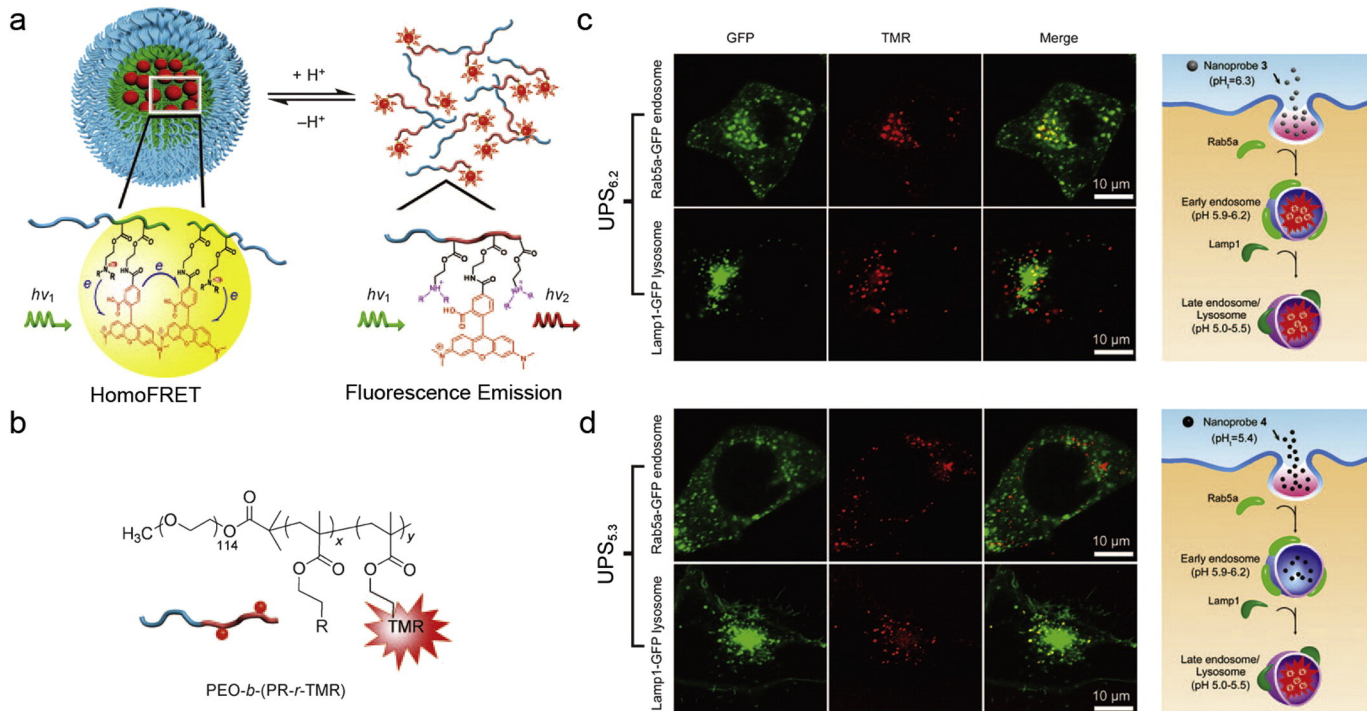


Fig. 1. (a) Schematic illustration of fluorescent UPS nanoprobe design. (b) Structures of the PEO-*b*-(PR-*r*-TMR) copolymers. Representative confocal microscopy images of activated UPS_{6.2} (c) and UPS_{5.3} (d) in cells with GFP-labeled early endosomes (top panel) and late endosomes/lysosomes (bottom panel) at 30 and 45 min, respectively; and schematic illustration of the selective activation of UPS_{6.2} in early endosomes (c, right panel) and UPS_{5.3} in late endosomes/lysosomes (d, right panel), respectively. Figures adapted from Ref. [36] with permission from Wiley-VCH.

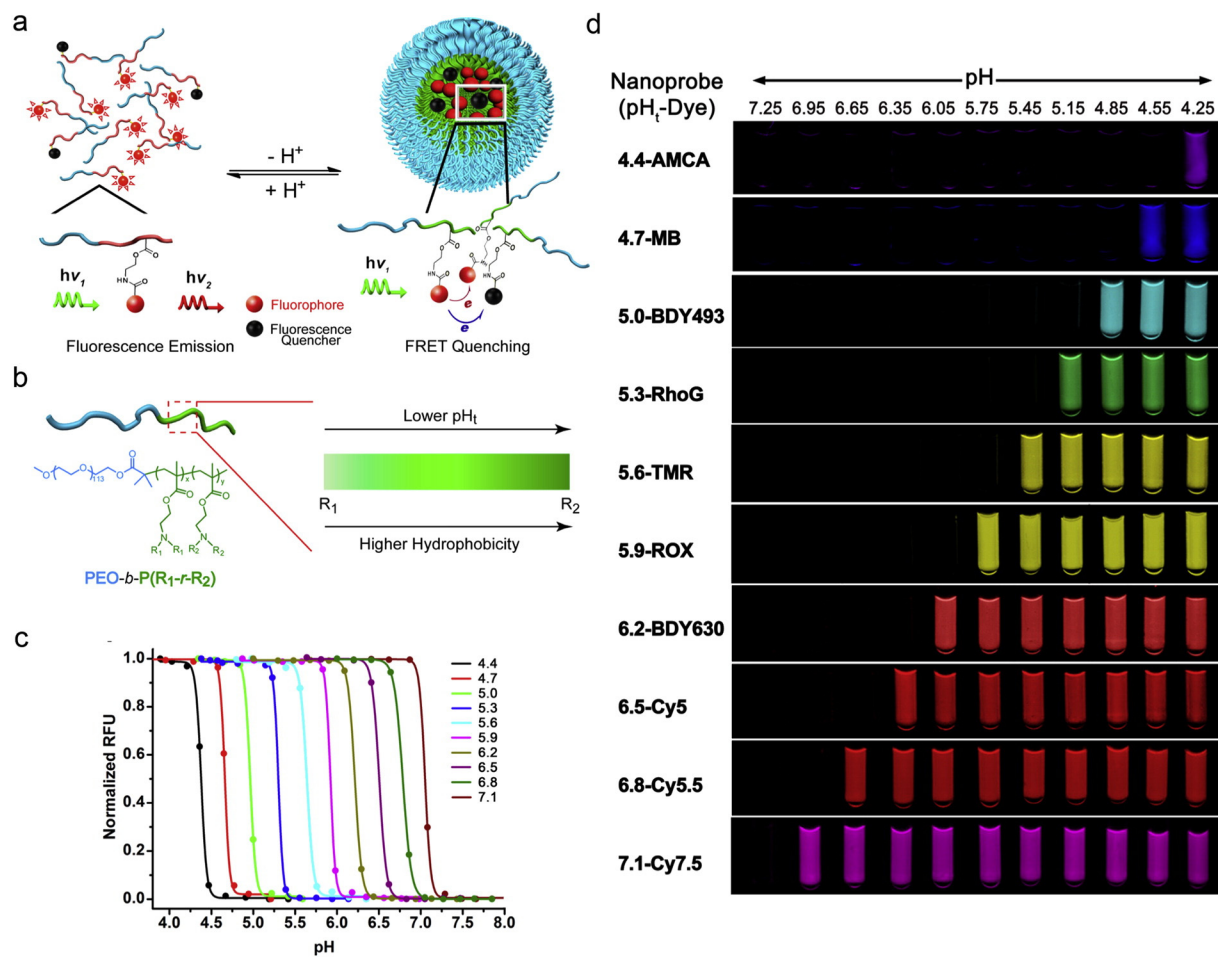


Fig. 2. (a) Schematic design of UPS nanoprobes with FQs. (b) A random copolymer strategy was used to achieve an operator predetermined control of the pH_t of UPS nanoprobes by the ability to continuously fine tune the hydrophobicity of PR segments. (c) Representative library of UPS nanoprobes with 0.3 pH increment covering the physiologic range of pH 4–7.4. (d) Exemplary UPS library consisting of 10 nanoprobes spanning a wide pH range (4–7.4) and large fluorescent emissions (400–820 nm). Figures adapted from Ref. [58] with permission from ACS Publications.

(<40 nm) like rhodamine and cyanine dyes. Fluorescence quenchers (FQs) are broadly used for activatable imaging probes [59–62]. They absorb radiative energy from fluorophores through hetero-FRET effect and dissipate it into heat. Dye-conjugated copolymers were mixed with FQ-conjugated copolymers with matched emission wavelengths into the same micelle core. FQs quench the fluorescence signals from the dyes at micelle state, but the energy transferring effect is diminished once micelles disassociate (Fig. 2a). Addition of FQs results in a high fluorescent activation of more than 50-fold signal amplification for fluorophores with large Stokes shifts (e.g., marina blue or PPO, $\Delta\lambda \geq 100$ nm), while no effect on the sharpness of pH transition was observed (Fig. 2c). This UPS library with each nanoprobe encoded with a different fluorophore provides a valuable toolkit to target a variety of physiological and pathological processes involving pH regulation. For example, in the low pH range, UPS_{4.4} can be used for detecting functional lysosome and hydrolase activity; in the intermediate range (pH 5.0–6.5), UPS nanoprobes are useful for studies of endosome maturation as well as drug delivery applications; UPS nanoprobes covering higher pH range (pH 6.5–7.1) can be an ideal fit for the study of acidic tumor microenvironment and early endosome formation and pH regulation (Fig. 2d).

3.2. Quantitative measurements: an 'always-ON/OFF-ON' design

To further pertain the ability to quantify the maturation process of endosomes, we improved the UPS nanoprobe design with a dual

fluorescence reporter for quantitative live-cell imaging. In this case, pH-insensitive 'always-ON' copolymers with one fluorescence encoding were employed to track intracellular distribution of UPS nanoprobes, and they were mixed with matched pH-activatable copolymers into the same micelle core. Initial attempts were focused at conjugating a dye (e.g., Cy3.5) on the terminal end of PEO to produce an 'always-ON' signal, however, the resulting nanoprobes showed binding to serum proteins, which made them unstable. To overcome this limitation, a hetero-FRET design using a pair of fluorophores was employed. In one example, BODIPY and Cy3.5 were used as donor and acceptor, respectively. Both dyes were conjugated separately to the PR segment of the copolymers. A mixture of both copolymers with two-fold donors (BODIPY) over acceptors (Cy3.5) allowed the hetero-FRET-induced fluorescence quenching of donor dye in the micelle state. When pH drops below the transition pH, micelle disassembly disrupts fluorescent energy transfer and the two fluorophores emit signals independently (Fig. 3a–b). Since cyanine dyes have small Stokes shift [63], to avoid the homo-FRET effect of Cy3.5 in the micelle state and make it an 'always-ON' signal, the weight fraction of Cy3.5-conjugated copolymer in the micelles were controlled as 40%. The resulting UPS nanoprobe showed sustained fluorescence in the Cy3.5 channel (always-ON) over a broad pH range, while a sharp pH response and high fluorescent activation (~30 fold) can still be observed in the BODIPY channel (OFF/ON, Fig. 3c). By using low dose (100 μ g/mL) always-ON/OFF-ON UPS_{6.2}, UPS_{5.3} and UPS_{4.4}, the progressive activation process of the nanoprobes in different endocytic organelles can be quantified by normalizing the

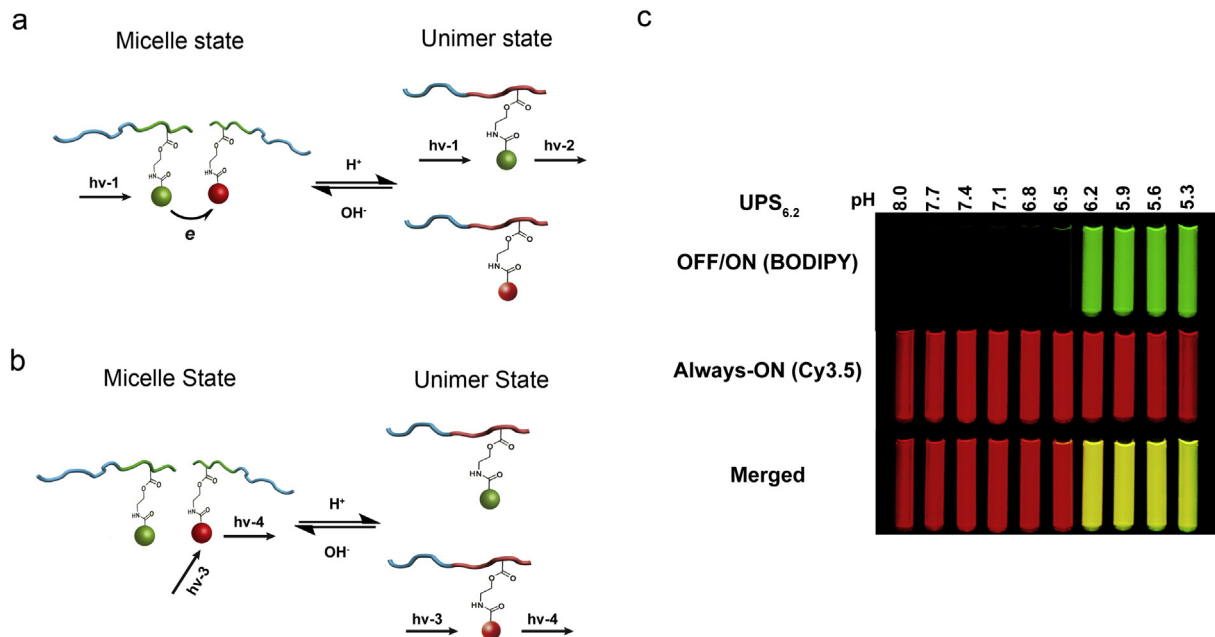


Fig. 3. (a-b) Schematic of the dual-reporter nanoprobe. In the micelle state, the always-ON dyes serve as the quencher for the OFF-ON fluorophores. When the micelle is disassembled, the always-ON and OFF-ON fluorophores can fluoresce independently. (c) Fluorescent images of test tubes filled with always-ON/OFF-ON UPS_{6.2} nanoprobe in buffers with different pH. Figures adapted from Ref. [64] with permission from Nature Publishing Group.

intensity of the fluorescent dots in the BODIPY channel by that in the Cy3.5 channel. This 'always-ON/OFF-ON' design not only allows the operator to track the localization of the nanoprobe, but may also provide a quantified method to characterize the acidification level of different cell lines.

3.3. Buffering effect – 'detecting and perturbing'

The pH sensitivity of UPS nanoprobe is based on the ionizable tertiary amine groups on the hydrophobic segment. Typical pH sensitive groups, including histidine, carboxylates, and sulfonamide-containing groups, also have various buffer capacity, and can be used as a 'proton sponge'. When these nanoprobe are internalized by cells, the buffer capacity may perturb intracellular or intra-organelle pH, which provides a unique opportunity to study intracellular pH regulation and how pH regulates cell signaling, metabolism and even cell death. This may also provide insights for studying the interaction between live cells and nanomaterials.

3.3.1. Physico-chemical and in vitro characterization

Previous studies have shown a sharp pH-responsive UPS nanoprobe library as a series of tunable fluorescence sensors for intracellular imaging. Actually, the pH-sensitive tertiary amine groups also provide the UPS nanoprobe library with a potent pH-tunable buffer capacity at a narrow pH interval across the physiological pH range from 4.0 to 7.4. Fig. 4a shows the pH titration curves of all UPS nanoprobe in the presence of 150 mM NaCl. Each nanoprobe buffered the pH of the polymer solution at their apparent pK_a as HCl was added. In contrast, chloroquine (CQ), a small molecule base that is commonly used to elevate lysosomal pH, showed a broad pH response in the range of pH 6 to 9 (pK_a = 8.3). Furthermore, polyethylenimine (PEI), a gold standard for nucleic acid delivery and also considered as a 'proton sponge', also behaved as a broad pH buffer [65]. Buffer capacity is determined by the following formula: $\beta = -dn_H^+/dpH$, where dn_H^+ is the quantity of added H⁺ and dpH is the associated pH change, which can be calculated from the pH titration curves. All nanoprobe showed strong and specific buffering effect around their pK_a, and the maximal β values can be more than 300-fold higher than CQ (Fig. 4b). This collection of UPS

nanoprobe thus provides a unique set of 'detecting and perturbing' toolkit for imaging and arresting early endosomes (E.E., 6.0–6.5) [57], late endosomes (L.E., 5.0–5.5) [57] and lysosomes (4.0–4.5) [4].

In the cell-based assays, UPS_{6.2}, UPS_{5.3} and UPS_{4.4} were selected as examples and showed dose-dependent and sustained pH plateaus at their pK_a, mimicking what they behave in the test tubes (Fig. 4c). However, the commonly used imaging dose 100 μ g/mL did not delay organelle acidification for any tested UPS nanoprobe. Furthermore, to quantify the acidification rates of endo/lysosomes, the average number of micelles per cell was measured based on the fluorescence intensity of internalized nanoprobe, and was divided by total cell number. The number of protons pumped per second for each organelle can then be calculated based on the number of amino groups per micelle and the average number of endosomes/lysosomes per cell (Table 1). The result is consistent with estimations [66–69] from literatures.

3.3.2. Coat protein dynamics

Coat proteins on endo/lysosomal membranes such as Rab5, Rab7, LAMP1 and LAMP2 facilitate targeted protein/cargo transports to these organelles, and they are also the biomarkers of organelle maturation. On the other hand, progressive acidification also indicates the transformation from early endosomes to lysosomes. Nanomaterials, such as UPS nanoprobe, which arrest endo/lysosomal pH may perturb the maturation of endosomes and also affect coat protein dynamics. To examine the consequences of UPS buffering of luminal pH on endosome protein coat maturation, UPS_{6.2} and UPS_{4.4} were selected to study the recruitment of the Rab5 GTPase, which is a discriminating feature of early endosome (pH 6.0–6.5) biogenesis [3], and LAMP2, which is a biomarker of lysosomes (pH 4.0–4.5) [4]. Fluorescent dextran was used as a temporally synchronized comparator that does not perturb luminal pH. UPS_{4.4} showed similar behavior as fluorescent dextran: over 60% colocalization with Rab5-positive/LAMP2-negative early endosomes in the first 15 min, and transitioned to a Rab5-negative/LAMP2-positive maturation state within 60 min. However, an unusual co-localization of UPS_{6.2}-positive endosomes with both Rab5- and LAMP2-positive vesicles was observed in a similar timeframe. The release of Rab5 was observed after 2 h when cells overcame the buffering capacity of UPS_{6.2}. These nanoprobe-enabled observations uncover a regulatory

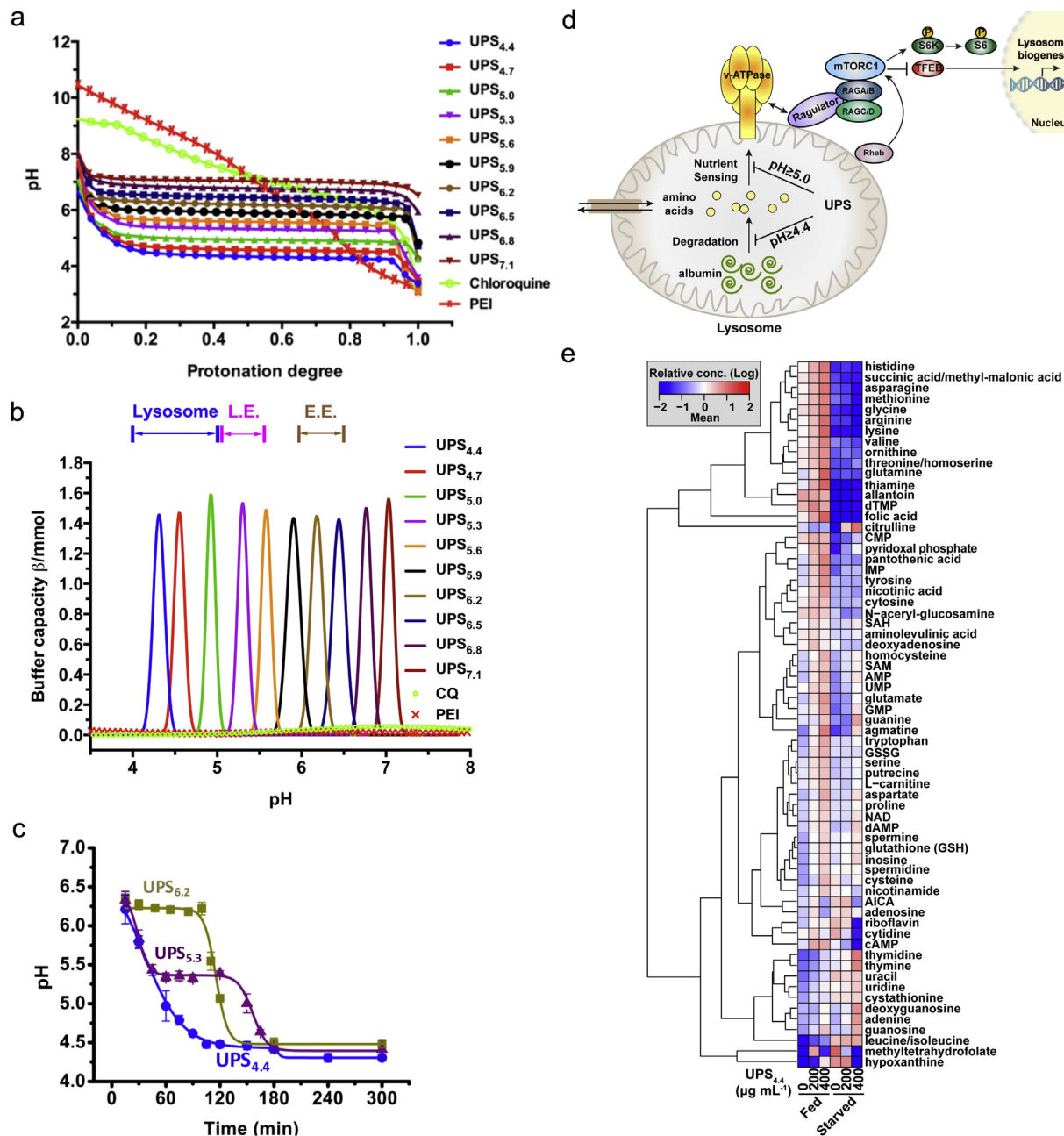


Fig. 4. (a) pH titration of each component of the UPS nanoprobe library. (b) Buffer capacity (β) for each component of the UPS library was plotted as a function of pH in the pH range of 4.0 to 7.4. (c) Real-time measurement of endo/lysosomal pH in HeLa cells treated with a dose of 1 mg/mL of UPS_{6.2}, UPS_{5.3} and UPS_{4.4}. (d) Working model of pH transitions required for free amino acid versus albumin-derived amino acid dependent activation of the mTORC1 signaling pathway. (e) A heatmap of relative abundance of the indicated metabolites under nutrient replete (fed) or deprived (starved) conditions. Cells were treated with UPS_{4.4} at the indicated doses.

Figures adapted from Ref. [64] with permission from Nature Publishing Group.

mechanism that recruits LAMP2 to nascent endo/lysosomes independent of the luminal pH and release Rab5 in a pH-dependent pathway.

3.3.3. Cell signaling and metabolism

Lysosomes are involved in degrading and recycling extracellular and intracellular materials through heterophagy and autophagy processes, respectively. More recently, they have also been identified as signaling organelles that mediate the nutrient-dependent activation of mammalian target of rapamycin complex 1 (mTORC1). In mammalian cells, it has been shown that mTORC1 is recruited to the surface of lysosomes in the presence of amino acids through a conformational change of v-ATPase [70] and Ragulator [7]. V-ATPase is also known as a main acidifier of endo/lysosomes. However, whether there is any connection

between the acidification of lysosomes and mTORC1 activation is currently unknown. UPS nanoprobes with strong and precisely controlled buffering capacity within a narrow pH range can act as a unique tool to examine the consequence of arresting luminal pH on endo/lysosome biology and the cell signaling events that flow through endo/lysosomes. UPS nanoprobes that discretely report and buffer at pH 6.2, 5.3, 5.0, 4.7 and 4.4 were selected to cover the functional pH range of endocytic organelles. Arresting pH to higher than 5.0 was sufficient to significantly delay and suppress the response of mTORC1 pathway to free amino acids. No obvious effect was observed from UPS_{4.7} and UPS_{4.4}. On the other hand, when bovine serum albumin (BSA) was used as a macromolecular nutrient source rather than free amino acids, UPS_{4.4} delayed mTORC1 activation in response to BSA as well as other UPS nanoprobes.

Table 1

Quantification of acidification rates of endocytic organelles by the UPS nanoparticles.
Table adapted from Ref. [64] with permission from Nature Publishing Group.

	[UPS] _{med} ($\mu\text{g/mL}$)	D_h/ξ (nm/mV) ^a	No. UPS/cell ($\times 10^2$) ^b	Plateau pH (mean \pm SD)	t_p (min) ^c	Rate ($\times 10^2/\text{s}$) ^d
UPS _{6,2}	100	44.3 \pm 1.2–16.6 \pm 1.8	4.7	n.d.	n.d.	n/a
	400		17	6.2 \pm 0.1	53	1.7
	1000		24	6.2 \pm 0.1	86	1.5
UPS _{5,3}	100	42.3 \pm 2.6/–0.7 \pm 0.1	4.6	n.d.	n.d.	n/a
	400		17	5.4 \pm 0.1	48	1.9
	1000		24	5.3 \pm 0.1	68	1.9
UPS _{4,4}	100	47.5 \pm 3.0/–1.1 \pm 0.2	4.4	n.d.	n.d.	n/a
	400		17	4.5 \pm 0.1	67	1.4
	1000		27	4.4 \pm 0.1	81	1.8

^a Hydrodynamic diameter (D_h) and zeta potential (ξ) were measured in the PBS buffer at pH 7.4.

^b Calculated based on 800 copolymer chains per micelle.

^c t_p is measured as the time interval where the pH was buffered at the plateau value.

^d The rate of proton accumulating in each endocytic organelle.

Given that UPS_{4,4} also largely suppresses the activity of cathepsin B and inhibits autophagic degradation of p62/SQSTM1 otherwise induced by serum-deprivation, we summarize these observations as distinct endo/lysosomal pH thresholds existing for free amino acids sensing ($\text{pH} < 5.0$) versus macromolecule degradation and sensing ($\text{pH} < 4.4$) (Fig. 4d).

Lysosomes recycle intracellular macromolecules and debris to produce metabolic intermediates and regulate energy metabolism [2]. Abnormal accumulation of large molecules, including lipids and glycoproteins in lysosomes are associated with metabolic disorders [71,72]. The highly selective perturbation of lysosomal acidification by UPS nanoprobes may be used to assess alteration of the metabolite pool associated with lysosomal malfunction. Liquid chromatography-triple quadrupole mass spectrometry (LC/MS/MS) was used to quantify intracellular metabolites. Under nutrient replete conditions, as the dose of UPS_{4,4} increased, the relative abundance of most amino acids increased, which is consistent with defects in lysosomal export of amino acids caused by pH arrest and/or an inhibition of amino acid consumption for protein synthesis. In nutrient deprived conditions, the loss of many essential amino acids including lysine, valine, methionine, and arginine is consistent with the inhibition of starvation-induced catabolism of macromolecules like albumin caused by UPS_{4,4} (Fig. 4e). Extensive metabolic profiling was done with higher dose of UPS_{6,2} UPS_{5,3}, UPS_{4,4} and baf A1. The response of UPS nanoprobes clustered nicely according to expectations associated with their pH clamping activity. Interestingly, comparing to nanoprobes and the vehicle controls, baf A1 induced distinct metabolic changes, which may reflect its broader intracellular targets. Together, there exist interplays between organelle acidification and metabolite pools, and proper lysosomal acidity is required for nutrient and energy homeostasis. Although further investigation

on mechanism of actions is needed, all these nanomaterials-enabled observations may unveil an unconventional way to study biological problem with nanotechnology.

3.3.4. Selective killing of cancer cells

Personalized therapy for cancer patients with specific genetic backgrounds is becoming more important to achieve broader therapeutic windows than the conventional cytotoxic drugs. Toward this goal, we recently identified a selective metabolic vulnerability of non-small cell lung cancer (NSCLC) cells with co-occurring oncogenic KRAS and suppressed LKB1 (liver kinase B1) activity, which results in their addiction to a lysosome-dependent supply of TCA cycle substrates for maintaining ATP production and mitochondria functions [73]. Genetic or chemical inhibition of v-ATPase activity has been shown to selectively induce apoptosis in this oncogenic background. Comparing to small molecule inhibitors, the buffering capacity of UPS nanoprobes may afford a cleaner environment to test whether lysosomal pH is sufficient to cause programmed cell death [8,74]. Normal (HBEC30KT) and tumor-derived (HCC4017) cell lines from the same patient were used to test the hypothesis, as well as an isogenic progression series with oncogenic KRAS and LKB1 suppression artificially introduced into the normal cell background [75]. UPS nanoprobes showed dose-dependent selective toxicity to bronchial epithelial cells with expression of oncogenic KRAS and inhibition of LKB1 (Fig. 5a–b). Moreover, UPS-induced programmed cell death was rescued by re-supplying cell-permeable TCA cycle substrates: methyl pyruvate and α -ketoglutarate (Fig. 5c). Together, these results indicate that selective vulnerability of KRAS/LKB1 co-mutant NSCLC cells to lysosomal pH arrest by UPS nanoprobes likely arises from addiction to lysosomal catabolism required for mitochondria health.

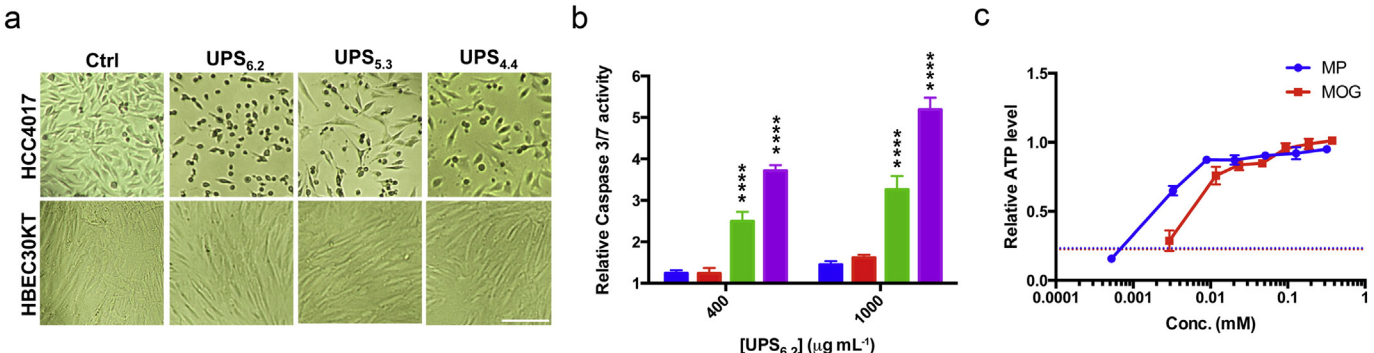


Fig. 5. (a) DIC images of HBEC30 KT and HCC4017 cells with and without exposure to UPS at their effective doses. Scale bar = 100 μm . (b) Caspase 3/7 activity in HBEC30KT (blue), HBEC30KT KP (red), HBEC30KT KPL (green) and HCC4017 (magenta) cells was measured 72 h after exposure to the indicated doses of UPS_{6,2}. $\alpha = 0.05$, $^{**}p < 0.01$, $^{***}p < 0.0001$. (c) Cellular ATP levels of HCC4017 treated with 1 mg/mL UPS_{6,2} for 72 h together with the indicated concentrations of methyl pyruvate (MP), dimethyl-2-oxoglutarate (MOG), or water (dash line). (For interpretation of the references to color in this figure legend, the reader is referred to the web version of this article.)
Figures adapted from Ref. [64] with permission from Nature Publishing Group.

4. Conclusions and future prospects

The maintenance of an appropriate pH gradient in the endocytic compartments is of great importance to their physiological functions. As a hallmark of endosomal maturation, the gradual acidification ensures the activation and inactivation of proteins and signaling molecules. Endosomes and lysosomes are extensions of plasma membranes in cell signaling and metabolism and play a fundamental role in many physiological and pathological conditions. Numerous studies have shown a highly complex and regulated endocytic pathway, however, specific mechanisms and concepts underlying the maturation of endocytic organelles into catabolic lysosomes needs to be benchmarked. Small molecular modulators such as chloroquine, NH₄Cl and Baf A1 have been commonly used for manipulation of endo/lysosomal acidification and luminal pH. However, these small molecules are membrane permeable and can target broader pH-dependent or even pH-independent activities. As a result, investigation of endosome/lysosome biology using these agents may suffer from complicated, non-specific effects on multiple acidic organelles (e.g., Golgi) [1].

pH-sensitive nanomaterials are playing an increasingly important role in various biomedical applications such as drug and gene delivery, diagnostic imaging, biosensing, and image-guided surgery. In this review, we describe the use of pH-sensitive nanoprobes for the fundamental studies of endosome and lysosome biology. One distinctive advantage of nanoprobes is that these nanoprobes are membrane-impermeable and can only enter cells through endocytosis. Another advantage that is unique to the UPS nanoprobes is the fast, tunable and amplified fluorescent signals at specific pH transitions comparing to the reported pH-sensitive probes (e.g., small molecular pH sensitive dyes [76], peptides [77,78], or photoelectron transfer (PeT) nanoprobes [79,80] with 10-fold signal change over 2 pH). A UPS library with 0.3 pH increment covering pH range from 4.0 to 7.4 affords an ideal toolkit for imaging subtle pH change in endocytic vesicles. Development of always-ON/OFF-ON UPS nanoprobes has extended their applications into quantitative imaging measurement of endo/lysosomal acidification rate. Recently identified strong buffering capacity of UPS nanoprobes further creates a 'detect and perturbation' strategy that is suitable for studying endocytic organelles and their luminal pH in various biological contexts. These nanoprobes should also be useful to investigate the "proton sponge" effect in drug and gene delivery, and offer much higher pH resolution than the conventional poly(ethyleneimines) [81] to investigate the most optimal pH range for endosomal escape and cytosolic delivery. The ultra-pH sensitive property of the UPS nanoparticles is a unique nanoscale property of stimuli-triggered supramolecular self-assembly systems, where nanoparticle transition or hydrophobic micellization renders all-or-none cooperativity that can be leveraged to amplify or switch signals [54]. Such self-assembly principles can potentially be extended to the development of other stimuli-responsive nanomaterials with a binary response to an external stimulus, and can offer new opportunities to investigating biology with an increased precision and sensitivity.

Acknowledgments

This work is supported by the National Institutes of Health (NIH) grants R01CA192221 (J.G.), R01CA71443 and R01CA176284 (M.A.W.), Cancer Prevention and Research Institute of Texas (CPRIT) grants RP140140 (J.G.), RP121067, RP110710 (M.A.W.), and the Welch Foundation grant I-1414 (M.A.W.). C.W. is a Howard Hughes Medical Institute (HHMI) International Student Research Fellow.

References

- [1] F.R. Maxfield, T.E. McGraw, Endocytic recycling, *Nat. Rev. Mol. Cell Biol.* 5 (2004) 121–132.
- [2] C. Settembre, A. Fraldi, D.L. Medina, A. Ballabio, Signals from the lysosome: a control centre for cellular clearance and energy metabolism, *Nat. Rev. Mol. Cell Biol.* 14 (2013) 283–296.
- [3] J. Huotari, A. Helenius, Endosome maturation, *EMBO J.* 30 (2011) 3481–3500.
- [4] J.R. Casey, S. Grinstein, J. Orlowski, Sensors and regulators of intracellular pH, *Nat. Rev. Mol. Cell Biol.* 11 (2010) 50–61.
- [5] S. Mukherjee, R.N. Ghosh, F.R. Maxfield, Endocytosis, *Physiol. Rev.* 77 (1997) 759–803.
- [6] C. De Duve, B. Pressman, R. Gianetto, R. Wattiaux, F. Appelmann, Tissue fractionation studies. 6. Intracellular distribution patterns of enzymes in rat-liver tissue, *Biochem. J.* 60 (1955) 604.
- [7] Y. Sancak, L. Bar-Peled, R. Zoncu, A.L. Markhard, S. Nada, D.M. Sabatini, Ragulator-rag complex targets mTORC1 to the lysosomal surface and is necessary for its activation by amino acids, *Cell* 141 (2010) 290–303.
- [8] A. Efeyan, W.C. Comb, D.M. Sabatini, Nutrient-sensing mechanisms and pathways, *Nature* 517 (2015) 302–310.
- [9] S. Pena-Llopis, S. Vega-Rubin-de-Celis, J.C. Schwartz, N.C. Wolff, T.A. Tran, L. Zou, X.J. Xie, D.R. Corey, J. Brugarolas, Regulation of TFEB and V-ATPases by mTORC1, *EMBO J.* 30 (2011) 3242–3258.
- [10] C. Settembre, R. Zoncu, D.L. Medina, F. Vetrini, S. Erdin, S. Erdin, T. Huynh, M. Ferron, G. Karsenty, M.C. Vellard, V. Fachinetti, D.M. Sabatini, A. Ballabio, A lysosome-to-nucleus signalling mechanism senses and regulates the lysosome via mTOR and TFEB, *EMBO J.* 31 (2012) 1095–1108.
- [11] H.T. McMahon, E. Boucrot, Molecular mechanism and physiological functions of clathrin-mediated endocytosis, *Nat. Rev. Mol. Cell Biol.* 12 (2011) 517–533.
- [12] J.A. Swanson, C. Watts, Macropinocytosis, *Trends Cell Biol.* 5 (1995) 424–428.
- [13] H. Stenmark, Rab GTPases as coordinators of vesicle traffic, *Nat. Rev. Mol. Cell Biol.* 10 (2009) 513–525.
- [14] M. Sardiello, M. Palmieri, A. di Ronza, D.L. Medina, M. Valenza, V.A. Gennarino, C. Di Malta, F. Donaudy, V. Embrione, R.S. Polishchuk, A gene network regulating lysosomal biogenesis and function, *Science* 325 (2009) 473–477.
- [15] C. Settembre, R. De Cegli, G. Mansueto, P.K. Saha, F. Vetrini, O. Visvikis, T. Huynh, A. Carissimo, D. Palmer, T.J. Klisch, TFEB controls cellular lipid metabolism through a starvation-induced autoregulatory loop, *Nat. Cell Biol.* 15 (2013) 647–658.
- [16] K.K. Huynh, S. Grinstein, Regulation of vacuolar pH and its modulation by some microbial species, *Microbiol. Mol. Biol. Rev.* 71 (2007) 452–462.
- [17] T.J. Jentsch, Clc chloride channels and transporters: from genes to protein structure, pathology and physiology, *Crit. Rev. Biochem. Mol. Biol.* 43 (2008) 3–36.
- [18] V. Marshansky, M. Futai, The V-type H⁺-ATPase in vesicular trafficking: targeting, regulation and function, *Curr. Opin. Cell Biol.* 20 (2008) 415–426.
- [19] E.J. Bowman, A. Siebers, K. Altendorf, Bafilomycins: a class of inhibitors of membrane ATPases from microorganisms, animal cells, and plant cells, *Proc. Natl. Acad. Sci. U. S. A.* 85 (1988) 7972–7976.
- [20] M. Huss, G. Ingenhorst, S. König, M. Gaßel, S. Dröse, A. Zeeck, K. Altendorf, H. Wieczorek, Concanamycin A, the specific inhibitor of V-ATPases, binds to the Vo subunit c, *J. Biol. Chem.* 277 (2002) 40544–40548.
- [21] N. Bayer, D. Schober, E. Prchla, R.F. Murphy, D. Blaas, R. Fuchs, Effect of bafilomycin A1 and nocodazole on endocytic transport in HeLa cells: implications for viral uncoating and infection, *J. Virol.* 72 (1998) 9645–9655.
- [22] G. Baravalle, D. Schober, M. Huber, N. Bayer, R.F. Murphy, R. Fuchs, Transferrin recycling and dextran transport to lysosomes is differentially affected by bafilomycin, nocodazole, and low temperature, *Cell Tissue Res.* 320 (2005) 99–113.
- [23] A. Van Weert, K.W. Dunn, H. Gueze, F.R. Maxfield, W. Stoorvogel, Transport from late endosomes to lysosomes, but not sorting of integral membrane proteins in endosomes, depends on the vacuolar proton pump, *J. Cell Biol.* 130 (1995) 821–834.
- [24] A. Yamamoto, Y. Tagawa, T. Yoshimori, Y. Moriyama, R. Masaki, Y. Tashiro, Bafilomycin A1 prevents maturation of autophagic vacuoles by inhibiting fusion between autophagosomes and lysosomes in rat hepatoma cell line, H-4-II-E cells, *Cell Struct. Funct.* 23 (1998) 33–42.
- [25] J.-H. Lee, W.H. Yu, A. Kumar, S. Lee, P.S. Mohan, C.M. Peterhoff, D.M. Wolfe, M. Martinez-Vicente, A.C. Massey, G. Sovak, Lysosomal proteolysis and autophagy require presenilin 1 and are disrupted by Alzheimer-related PS1 mutations, *Cell* 141 (2010) 1146–1158.
- [26] B.A. Webb, M. Chimenti, M.P. Jacobson, D.L. Barber, Dysregulated pH: a perfect storm for cancer progression, *Nat. Rev. Cancer* 11 (2011) 671–677.
- [27] D.S. Rao, S.V. Bradley, P.D. Kumar, T.S. Hyun, D. Saint-Dic, K. Oravecz-Wilson, C.G. Kleer, T.S. Ross, Altered receptor trafficking in huntingtin interacting protein 1-transformed cells, *Cancer Cell* 3 (2003) 471–482.
- [28] C.E. Fleming, F.M. Mar, F. Franquinho, M.J. Saraiava, M.M. Sousa, Transthyretin internalization by sensory neurons is megalin mediated and necessary for its neuritogenic activity, *J. Neurosci.* 29 (2009) 3220–3232.
- [29] E. Trushina, R.D. Singh, R.B. Dyer, S. Cao, V.H. Shah, R.G. Parton, R.E. Pagano, C.T. McMurray, Mutant huntingtin inhibits clathrin-independent endocytosis and causes accumulation of cholesterol in vitro and in vivo, *Hum. Mol. Genet.* 15 (2006) 3578–3591.
- [30] R.A. Nixon, Endosome function and dysfunction in Alzheimer's disease and other neurodegenerative diseases, *Neurobiol. Aging* 26 (2005) 373–382.
- [31] D.G. Isom, V. Sridharan, R. Baker, S.T. Clement, D.M. Smalley, H.G. Dohlman, Protons as second messenger regulators of G protein signaling, *Mol. Cell* 51 (2013) 531–538.
- [32] A. Hurtado-Lorenzo, M. Skinner, J. El Annan, M. Futai, G.H. Sun-Wada, S. Bourgois, J. Casanova, A. Wildeman, S. Bechoua, D.A. Ausiello, D. Brown, V. Marshansky, V-ATPase interacts with ARNO and Arf6 in early endosomes and regulates the protein degradative pathway, *Nat. Cell Biol.* 8 (2006) 124–136.
- [33] A.M. Tartakoff, Perturbation of vesicular traffic with the carboxylic ionophore monensin, *Cell* 32 (1983) 1026–1028.
- [34] D. Schmaljohann, Thermo- and pH-responsive polymers in drug delivery, *Adv. Drug Deliv. Rev.* 58 (2006) 1655–1670.

[35] Y. Bae, S. Fukushima, A. Harada, K. Kataoka, Design of environment-sensitive supramolecular assemblies for intracellular drug delivery: Polymeric micelles that are responsive to intracellular pH change, *Angew. Chem.* 115 (2003) 4788–4791.

[36] K. Zhou, Y. Wang, X. Huang, K. Luby-Phelps, B.D. Sumer, J. Gao, Tunable, ultrasensitive pH-responsive nanoparticles targeting specific endocytic organelles in living cells, *Angew. Chem. Int. Ed.* 50 (2011) 6109–6114.

[37] E.S. Lee, Z. Gao, Y.H. Bae, Recent progress in tumor pH targeting nanotechnology, *J. Control. Release* 132 (2008) 164–170.

[38] M.A.C. Stuart, W.T. Huck, J. Genzer, M. Müller, C. Ober, M. Stamm, G.B. Sukhorukov, I. Szleifer, V.V. Tsukruk, M. Urban, Emerging applications of stimuli-responsive polymer materials, *Nat. Mater.* 9 (2010) 101–113.

[39] H. Yin, E.S. Lee, D. Kim, K.H. Lee, K.T. Oh, Y.H. Bae, Physicochemical characteristics of pH-sensitive poly (L-histidine)-b-poly (ethylene glycol)/poly(L-lactide)-b-poly (ethylene glycol) mixed micelles, *J. Control. Release* 126 (2008) 130–138.

[40] E.S. Lee, K. Na, Y.H. Bae, Polymeric micelle for tumor pH and folate-mediated targeting, *J. Control. Release* 91 (2003) 103–113.

[41] E.S. Lee, H.J. Shin, K. Na, Y.H. Bae, Poly (L-histidine)-PEG block copolymer micelles and pH-induced destabilization, *J. Control. Release* 90 (2003) 363–374.

[42] E.S. Lee, Z. Gao, D. Kim, K. Park, I.C. Kwon, Y.H. Bae, Super pH-sensitive multifunctional polymeric micelle for tumor pH specific TAT exposure and multidrug resistance, *J. Control. Release* 129 (2008) 228–236.

[43] E.S. Lee, K. Na, Y.H. Bae, Doxorubicin loaded pH-sensitive polymeric micelles for reversal of resistant MCF-7 tumor, *J. Control. Release* 103 (2005) 405–418.

[44] V.A. Sethuraman, K. Na, Y.H. Bae, pH-responsive sulfonamide/PEI system for tumor specific gene delivery: an *in vitro* study, *Biomacromolecules* 7 (2006) 64–70.

[45] V.A. Sethuraman, Y.H. Bae, TAT peptide-based micelle system for potential active targeting of anti-cancer agents to acidic solid tumors, *J. Control. Release* 118 (2007) 216–224.

[46] J.-Z. Du, C.-Q. Mao, Y.-Y. Yuan, X.-Z. Yang, J. Wang, Tumor extracellular acidity-activated nanoparticles as drug delivery systems for enhanced cancer therapy, *Biotechnol. Adv.* 32 (2014) 789–803.

[47] Y. Bae, S. Fukushima, A. Harada, K. Kataoka, Design of environment-sensitive supramolecular assemblies for intracellular drug delivery: polymeric micelles that are responsive to intracellular pH change, *Angew. Chem. Int. Ed.* 42 (2003) 4640–4643.

[48] H.S. Yoo, E.A. Lee, T.G. Park, Doxorubicin-conjugated biodegradable polymeric micelles having acid-cleavable linkages, *J. Control. Release* 82 (2002) 17–27.

[49] E.R. Gillies, J.M.J. Frechet, pH-responsive copolymer assemblies for controlled release of doxorubicin, *Bioconjug. Chem.* 16 (2005) 361–368.

[50] E.R. Gillies, T.B. Jonsson, J.M. Frechet, Stimuli-responsive supramolecular assemblies of linear-dendritic copolymers, *J. Am. Chem. Soc.* 126 (2004) 11936–11943.

[51] J.Z. Du, T.M. Sun, W.J. Song, J. Wu, J. Wang, A tumor-acidity-activated charge-conversional nanogel as an intelligent vehicle for promoted tumoral-cell uptake and drug delivery, *Angew. Chem.* 122 (2010) 3703–3708.

[52] R.M. Clegg, Fluorescence resonance energy transfer, *Curr. Opin. Biotechnol.* 6 (1995) 103–110.

[53] P. Wu, L. Brand, Resonance energy transfer: methods and applications, *Anal. Biochem.* 218 (1994) 1–13.

[54] Y. Li, T. Zhao, C. Wang, Z. Lin, G. Huang, B.D. Sumer, J. Gao, Molecular basis of cooperativity in pH-triggered supramolecular self-assembly, *Nat. Commun.* (2016) (in press).

[55] Y. Li, Z. Wang, Q. Wei, M. Luo, G. Huang, B.D. Sumer, J. Gao, Non-covalent interactions in controlling pH-responsive behaviors of self-assembled nanosystems, *Polym. Chem.* (2016), <http://dx.doi.org/10.1039/C6PY01104G>.

[56] K. Zhou, H. Liu, S. Zhang, X. Huang, Y. Wang, G. Huang, B.D. Sumer, J. Gao, Multicolored pH-tunable and activatable fluorescence nanoplatform responsive to physiologic pH stimuli, *J. Am. Chem. Soc.* 134 (2012) 7803–7811.

[57] O.A. Weisz, Acidification and protein traffic, *Int. Rev. Cytol.* 226 (2003) 259–319.

[58] X. Ma, Y. Wang, T. Zhao, Y. Li, L.-C. Su, Z. Wang, G. Huang, B.D. Sumer, J. Gao, Ultra-pH sensitive nanoprobe library with broad pH tunability and fluorescence emissions, *J. Am. Chem. Soc.* 136 (2014) 11085–11092.

[59] G. Blum, S.R. Mullins, K. Keren, M. Fonovič, C. Jedeszko, M.J. Rice, B.F. Sloane, M. Bogyo, Dynamic imaging of protease activity with fluorescently quenched activity-based probes, *Nat. Chem. Biol.* 1 (2005) 203–209.

[60] S. Lee, J.H. Ryu, K. Park, A. Lee, S.-Y. Lee, I.-C. Youn, C.-H. Ahn, S.M. Yoon, S.-J. Myung, D.H. Moon, Polymeric nanoparticle-based activatable near-infrared nanosensor for protease determination *in vivo*, *Nano Lett.* 9 (2009) 4412–4416.

[61] J. Levi, S.R. Kothapalli, T.-J. Ma, K. Hartman, B.T. Khuri-Yakub, S.S. Gambhir, Design, synthesis, and imaging of an activatable photoacoustic probe, *J. Am. Chem. Soc.* 132 (2010) 11264–11269.

[62] D. Maxwell, Q. Chang, X. Zhang, E.M. Barnett, D. Piwnica-Worms, An improved cell-penetrating, caspase-activatable, near-infrared fluorescent peptide for apoptosis imaging, *Bioconjug. Chem.* 20 (2009) 702–709.

[63] J.O. Escobedo, O. Rusin, S. Lim, R.M. Strongin, NIR dyes for bioimaging applications, *Curr. Opin. Chem. Biol.* 14 (2010) 64–70.

[64] C. Wang, Y. Wang, Y. Li, B. Bodermann, T. Zhao, X. Ma, G. Huang, Z. Hu, R.J. DeBerardinis, M.A. White, A nanobuffer reporter library for fine-scale imaging and perturbation of endocytic organelles, *Nat. Commun.* 6 (2015).

[65] J. Suh, H.-J. Paik, B.K. Hwang, Ionization of poly(ethylenimine) and poly(allylamine) at various pHs, *Bioorg. Chem.* 22 (1994) 318–327.

[66] D.W. Deamer, A. Kleinzeller, D.M. Fambrough, *Membrane Permeability: 100 Years Since Ernest Overton*, Academic Press, San Diego, CA, USA, 1999.

[67] R.L. Cross, V. Muller, The evolution of A-, F-, and V-type ATP synthases and ATPases: reversals in function and changes in the H⁺/ATP coupling ratio, *FEBS Lett.* 576 (2004) 1–4.

[68] H. Imamura, M. Nakano, H. Noji, E. Muneyuki, S. Ohkuma, M. Yoshida, K. Yokoyama, Evidence for rotation of V1-ATPase, *Proc. Natl. Acad. Sci. U.S.A.* 100 (2003) 2312–2315.

[69] J.S. Rodman, P.D. Stahl, S. Gluck, Distribution and structure of the vacuolar H⁺-ATPase in endosomes and lysosomes from LLC-PK1 cells, *Exp. Cell Res.* 192 (1991) 445–452.

[70] R. Zoncu, L. Bar-Peled, A. Efeyan, S. Wang, Y. Sancak, D.M. Sabatini, mTORC1 senses lysosomal amino acids through an inside-out mechanism that requires the vacuolar H⁺-ATPase, *Science* 334 (2011) 678–683.

[71] C. De Duve, The lysosome turns fifty, *Nat. Cell Biol.* 7 (2005) 847–849.

[72] T. Yeung, B. Ozdamar, P. Paroutis, S. Grinstein, Lipid metabolism and dynamics during phagocytosis, *Curr. Opin. Cell Biol.* 18 (2006) 429–437.

[73] H.S. Kim, S. Mendiratta, J. Kim, C.V. Pecot, J.E. Larsen, I. Zubovych, B.Y. Seo, J. Kim, B. Eskioçak, H. Chung, E. McMillan, S. Wu, J. De Brabander, K. Komurov, J.E. Toombs, S. Wei, M. Peyton, N. Williams, A.F. Gazdar, B.A. Posner, R.A. Brekken, A.K. Sood, R.J. Deberardinis, M.G. Roth, J.D. Minna, M.A. White, Systematic identification of molecular subtype-selective vulnerabilities in non-small-cell lung cancer, *Cell* 155 (2013) 552–566.

[74] C.-S. Zhang, B. Jiang, M. Li, M. Zhu, Y. Peng, Y.-L. Zhang, Y.-Q. Wu, T.Y. Li, Y. Liang, Z. Lu, The lysosomal V-ATPase-Ragulator complex is a common activator for AMPK and mTORC1, acting as a switch between catabolism and anabolism, *Cell Metab.* 20 (2014) 526–540.

[75] R.D. Ramirez, S. Sheridan, L. Girard, M. Sato, Y. Kim, J. Pollack, M. Peyton, Y. Zou, J.M. Kurie, J.M. DiMaio, Immortalization of human bronchial epithelial cells in the absence of viral oncogene, *Cancer Res.* 64 (2004) 9027–9034.

[76] Y. Urano, D. Asanuma, Y. Hama, Y. Koyama, T. Barrett, M. Kamiya, T. Nagano, T. Watanabe, A. Hasegawa, P.L. Choyke, Selective molecular imaging of viable cancer cells with pH-activatable fluorescence probes, *Nat. Med.* 15 (2009) 104–109.

[77] N.T. Viola-Villegas, S.D. Carlin, E. Ackerstaff, K.K. Sevak, V. Divilov, I. Serganova, N. Kruchevsky, M. Anderson, R.G. Blasberg, O.A. Andreev, D.M. Engelman, J.A. Koutcher, Y.K. Reshetnyak, J.S. Lewis, Understanding the pharmacological properties of a metabolic PET tracer in prostate cancer, *Proc. Natl. Acad. Sci. U.S.A.* 111 (2014) 7254–7259.

[78] D. Weerakkody, A. Moshnikova, M.S. Thakur, V. Moshnikova, J. Daniels, D.M. Engelman, O.A. Andreev, Y.K. Reshetnyak, Family of pH (low) insertion peptides for tumor targeting, *Proc. Natl. Acad. Sci. U.S.A.* 110 (2013) 5834–5839.

[79] Y. Diaz-Fernandez, F. Foti, C. Mangano, P. Pallavicini, S. Patroni, A. Perez-Gramatges, S. Rodriguez-Calvo, Micelles for the self-assembly of “off-on-off” fluorescent sensors for pH windows, *Chemistry* 12 (2006) 921–930.

[80] S. Uchiyama, K. Iwai, A.P. da Silva, Multiplexing sensory molecules map protons near micellar membranes, *Angew. Chem. Int. Ed.* 47 (2008) 4667–4669.

[81] A. von Harpe, H. Petersen, Y. Li, T. Kissel, Characterization of commercially available and synthesized polyethylenimines for gene delivery, *J. Control. Release* 69 (2000) 309–322.